Engineering Chemistry
ISSN: 2813-6535, Vol. 2, pp 35-41
doi:10.4028/p-1z7h01

Submitted: 2022-07-29
Revised: 2022-10-28
Accepted: 2022-11-10
Online: 2023-05-16

Synthesis and Electrochemical Properties of ZnO/ Activated Carbon from Vetiver Distillation Waste

Rafli Eghbal Haraki[1,a], Arenst Andreas Arie[2,b], Ratna Frida Susanti[2,c], Haryo Satriya Oktaviano[3,d], and Agung Nugroho[1,e*.]

[1]Department of Chemical Engineering, Faculty of Industrial Technology, Universitas Pertamina, Jakarta, Indonesia

[2]Chemical Engineering Department, Industrial Technology Faculty, 40141 Parahyangan Catholic University, Ciumbuleuit 94, Bandung, Indonesia

[3]Research and Technology Innovation, PT. Pertamina (Persero), Jakarta, 12950, Indonesia

[a]102318029@student.universitaspertamina.ac.ad, [b]arenst@unpar.ac.id, [c]santi@unpar.ac.id, [d]haryo.oktaviano@pertamina.com, [e]agung.n@universitaspertamina.ac.id
Corresponding Author: Agung Nugroho

Keywords: vetiver root waste, zinc oxide, impregnation, activated carbon, cyclic voltammetry, galvanostatic charge-discharge.

Abstract. The addition of zinc oxide (ZnO) as impregnation for activated carbon (AC) with the hydrothermal method has been performed in this research. Vetiver distillation waste has been used as a precursor for activated carbon synthesized with pyrolisis methods. Carbon is activated by a chemical process using KOH. Enhancement of amorph structure and function group by addition of zinc oxide has been characterized by Raman Spectroscopy, Fourier Transform Infra-Red (FT-IR), and X-Ray Diffraction (XRD). Furthermore, cyclic voltammetry (CV) and galvanostatic charge-discharge (GCD) has been done to show the electrochemical properties enhancement of the ZnO/AC compared to pristine AC. At the current density of 1 A/g, the specific capacitance of VRW-ACM has a value of 277 F/g. After the impregnation process, the specific capacitance of VRW-ACM-ZnO has been improved by 44.4% compared to VRW-ACM. The result showed that the activated carbon-based vetiver root waste impregnated with ZnO has the potential to be applied as supercapacitors electrodes.

Introduction

Nowadays, the use of electric vehicles is increasing rapidly. This development is also in line with the rapid distribution of electrical energy. Public electric vehicle charging stations are increasingly needed all over the globe. However, many charging stations in developing countries still rely on fossil fuel resources. In the future, solar cell-based charging stations will become promising. Solar cell-based charging stations require storage devices with a large power density and fast charge-discharge times. Supercapacitors are considered suitable to answer these needs [1]. Supercapacitors have been widely developed as electrical energy storage. The advantages of supercapacitors are high life cycle, high specific power delivery, and fast charge-discharge compared to batteries. Supercapacitors have the drawback of small energy density. Increasing energy density can be done using electrode materials with high capacitance, and optimizing the supercapacitor structure [2]. Electrode materials are one of the main factors for determining the performance of supercapacitors and have become the focus of ongoing research. Activated carbon is the most widely studied to be used as a supercapacitor electrode material. Especially in developing environmentally friendly activated carbon materials, one of which is biomass-based. The highest specific capacitance value was recorded at 374 F/g from activated carbon-derived biomass [3]. Vetiver root waste is one of the biomasses that has the potential to be converted to activated carbon (AC) as electrode material due to its high cellulose (43%) and lignin (37.8%) content. Previous research shows the potential of activated carbon based on vetiver root waste to be applied as an electrode due to its high surface area of 552.9 m^2/g [4]. Of the many metal oxides used to improve the electrochemical performance of electrode materials, ZnO has attracted much researchers because it has large theoretical capacitance

values (0.5 A/g current density or 340 F/g). ZnO is low in price, environmentally friendly, and easy to obtain. [5]. Previous studies by Li et al. obtained superior cyclic stability (99% in 1000 cycles) with the ratio of AC/ZnO = 1:2 [6]. This study used vetiver root waste as a supercapacitor electrode with zinc oxide impregnation to utilize vetiver root waste. This study used characterization and electrochemical analysis such as FTIR, XRD, Raman Spectroscopy, CV, and GCD. Thus, this study is expected to produce materials with high specific capacitance so that they can become an alternative to supercapacitor electrode materials.

Material and Method

Materials. Pottasium hydroxide (Merck), Zinc Oxide (ROFA Laboratory Centre), Sodium hydroxide (Merck), Sulphuric acid (Mallinckrodt), Nafion (Merck). All used regents were in analytic grade.

Synthesis of Activated Carbon. Vetiver root waste is obtained from the essential oil home industry in Garut, West Java, Indonesia. All other reagents were analytical grade, and the solution was prepared using double-distilled water. Vetiver root waste is cleaned with water to remove the impurities and dried in the oven at 110°C for 24 h. Dry vetiver root waste is ground with a ball mill and filtered with 100 mesh. The powdered material was pre-carbonized for 1 h at 400°C in a muffle furnace to produce pyrochar [7]. The pre-carbonized powder was mixed with KOH at a mass ratio for C/KOH = 1:3. The mixture was activated in N_2 to obtain the vetiver root waste-activated carbon at 800°C for 2 h.

Synthesis of ZnO/Activated Carbon. The ZnO/AC composite was synthesized with the hydrothermal method. ZnO solution was made by dissolving 0.05 g ZnO powder in 120 ml double distilled water. 0.1 g of pyrochar was dispersed in ZnO solution and stirred for 30 min. Then mixer was transferred into a Teflon-lined autoclave with a volume of 200 mL and heated for 4 h at 150°C. After multiple washing with double distilled water, ZnO/AC composite was dried in the oven for 8h at 70°C, and the ZnO/AC sample was obtained.

Characterization. Functional groups were analyzed by FT-IR Thermo Scientific iS5 in 600-4000 cm^{-1} wavelength. Crystal structures were characterized by X-Ray Diffraction Olympus BTX II Benchtop using Co-Kα radiation and scanning speed of 0.5°/min. The defect of the material was determined by Raman spectra Horiba spectrometry (LabRAM HR Evolution Raman Microscope) at a wavelength of 532 nm and 1800 g/mm.

Electrochemical Measurement. Active material (AC or ZnO/AC) as much as 1.6 mg were mixed with 0.5 ml of isopropanol and then sonicated for 15 min to form an ink. A 0.6 µl ink was dropped to a glassy carbon electrode and coated with 0.3 µl nafion. The complete method of the working electrode preparation can be seen in our previous report [8]. By using aqueous electrolyte Na_2SO_4 1 M concentration, the three-electrode system was assembled with the reference electrode (Ag/AgCl), working electrode (glassy carbon), and counter electrode (Pt wire). Cyclic Voltammetry was measured within 5, 10, 20, 50, and 100 mV/s. GCD was measured within 0.5 to 10 A/g.

Result and Discussion.

The FTIR result (Fig.1) identified the O-H stretching functional group at wavenumber 3444 cm-1. This group was identified due to the presence of KOH activators that have not disappeared even after intensive washing [9], [10]. The O-H stretching group is also indicated by phenol commonly found in activated carbon [11]. The stretching C-H group was identified at wavenumber 2922 cm-1, and the intensity in the C-H group was not very significant due to activation at high temperatures [12]. The C=C stretching group was identified in wavenumber 1636 cm^{-1}. This group also indicates the loss of the oxygen group due to high-temperature treatment [6]. For the VRW-ACM ZnO sample, the Zn-O group was not identified because the group was read on a wavenumber of 400 cm^{-1}. Another thing that explains the absence of Zn-O is due to the low content of impregnation. At a ZnO: AC mass ratio of 0.5 grams, ZnO enters the pore and leaves no deposition on the surface, making it challenging to read FTIR [13].

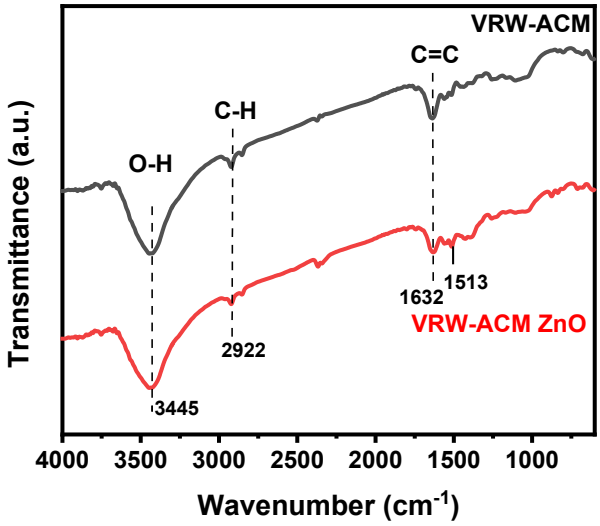

Fig.1. FTIR test result for VRW-ACM and VRW-ACM ZnO

Raman analysis (Fig.2a) showed the presence of bands at 1349 and 1578 cm^{-1} indicating D-band and G-band. The defect degrees of activated carbon samples (VRW-ACM) and ZnO-impregnated activated carbon samples (VRW-ACM ZnO) were calculated by comparing the D-band and G-band intensities. The degree of defect of VRW-ACM and the VRW-ACM ZnO was calculated by comparing the D-band and G-band intensities as written in Fig.2. In the VRW-ACM ZnO sample, the I_D/I_G value decreased compared to VRW-ACM. This result indicates that graphite carbon levels are higher after adding ZnO. The higher degree of graphitization can result from the catalytic graphitization process, which usually occurs in carbon pyrolysis in the presence of metal oxide [14]. In these cases, zinc oxide leads to the conversion of carbon structure into the ordered graphitic structure. This shows in the low I_D/I_G value of VRM-ACM-ZnO compared to pristine VRM-ACM. These results correspond to previous tests comparing the impregnation of ZnO to activated carbon with commercial activated carbon increasing the crystallinity value [15]. In addition, there is no reaction to the impregnation of zinc oxide into activated carbon so that it does not damage the structure of the sample. The XRD result of activated carbon before and after ZnO impregnation can be seen in Fig.2b. The XRD pattern of VRW-ACM shows peaks at 26.58° and 44.26°, which is in agreement with the XRD pattern of carbon materials [16]. After ZnO impregnation, an unnoticeable peak can be seen in the result. This result indicates that ZnO is only impregnated in the carbon structure without entering into the structure of carbon. The similar result has also been observed in the previous research done by Aljeboree et al [17].

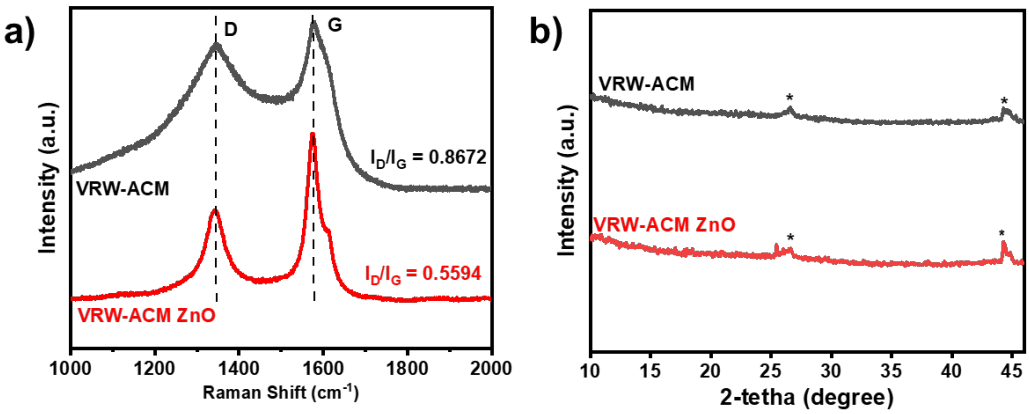

Fig.2. Raman Spectroscopy (a) and XRD analysis (b) result of VRW-ACM and VRW-ACM ZnO

The sample VRW-ACM and VRW-ACM-ZnO was then analyzed by CV to see the electrochemical mechanism in the three-electrode system (Fig. 3). The CV curve of VRW-ACM shows a symmetrical curve in various scan rate, which indicates the EDLC mechanism (Fig. 3a). The curve also shows that there is no reduction or oxidation reaction, which agrees with the concept of the EDLC supercapacitor mechanism, which only occurs on surfaces [18]. The storage mechanism of EDLC is a reversible surface phenomenon involving the adsorption and desorption of Na+ ions from the electrolyte. After the impregnation of ZnO into the carbon structure, the shape of the curve changes, indicating the pseudocapacitance mechanism [19]. Further, at a scan rate of 10 mV/s, the comparison of CV between before and after ZnO addition shows that VRM-ACM-ZnO has a more significant CV curve area (Fig. 3c). The large area of the CV curve might indicate the larger specific capacitance of VRW-ACM-ZnO compared to the pristine VRW-ACM sample.

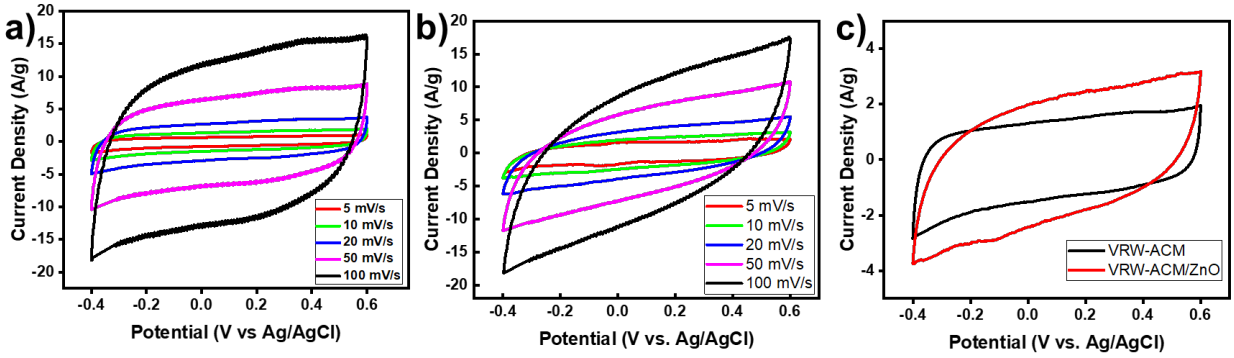

Fig.3. CV test result for (a) VRW-ACM (b) VRW-ACM ZnO (c) comparison at scan rate 10 mV/s

GCD analysis was performed to quantify the specific capacitance of the as-synthesized material. Both samples show that the curve forms the same charge-discharge manner. The GCD result of pristine activated carbon (Fig. 4a) shows the symmetrical triangle that results from the EDLC mechanism [20]. This result differs from the GCD result of ZnO impregnated samples (Fig. 4b), which shows that the discharge time is longer than the charging time. The curvature at the end indicates a redox reaction between ZnO and electrolyte ions. This phenomenon shows the combined mechanism, namely EDLC on charge and pseudocapacitance on discharge [21]. Table 1 shows the calculated value of specific capacitance from GCD analysis. It can be seen that after adding ZnO, the specific capacitance of the materials increases all current densities.

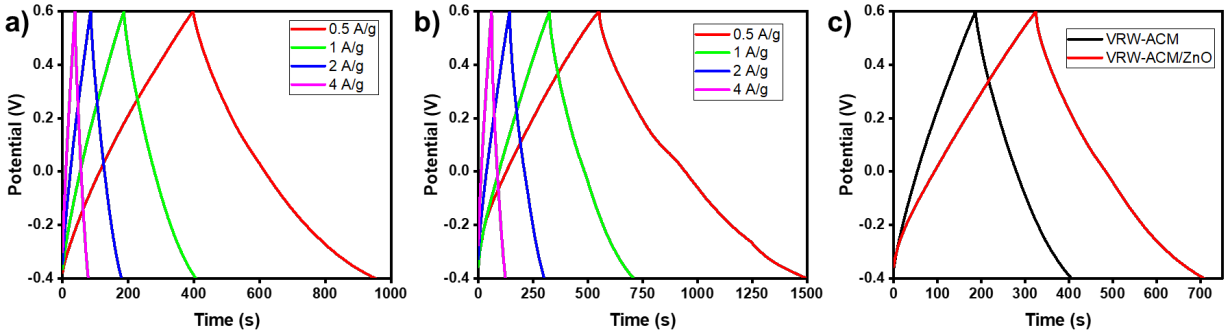

Fig.4. GCD test result for (a) VRW-ACM, (b) VRW-ACM ZnO and (c) comparison at current density 1A/g

Table 1. Capacitance for VRW-ACM and VRW-ACM ZnO

Sample	Current Density (A/g)	Specific Capacitance (F/g)	Increase of Capacitance
VRW-ACM	0.5	277	-
	1	218	-
	2	186	-
	4	160	-
VRW-ACM-ZnO	0.5	400	44%
	1	383	75%
	2	314	66%
	4	248	55%

The GCD cyclability test was carried out at 4 A/g current density to determine the retention of the VRW-ACM-ZnO material after being cycled 50 times (Fig.5). The result was reduced from 246 F/g to 239 F/g after 50 cycles. In the 50 cycles, there is relatively good stability. An insignificant and still higher decline than VRW-ACM before impregnation proves that VRW-ACM ZnO has the potential to be used as an electrode for supercapacitors.

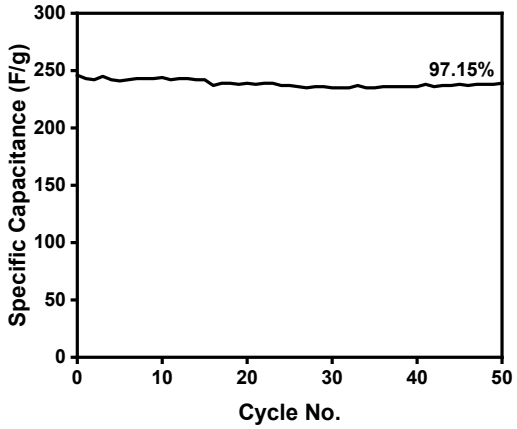

Fig.5. Cycle Performance of VRW-ACM ZnO

Conclusion

Vetiver root waste left over from essential oil distillation can be a precursor to the manufacture of activated carbon by pyrolysis and hydrothermal pre-carbonization methods followed by activation with KOH. The FTIR, Raman, and XRD analysis show that zinc oxide impregnation was successfully carried into activated carbon. The decrease in defects in Raman analysis reflects the graphitization of carbon materials into the graphitic structure. The CV and GCD analysis showed an increase in specific capacitance in each sample. This result suggests that activated carbon material was successfully impregnated with zinc oxide and has the potential to be used as an electrode for supercapacitors.

References

[1] X. Jiang, L. Zhao, Y. Cheng, S. Wei, and Y. Jin, “Optimal configuration of electric vehicles for charging stations under the fast power supplement mode,” *J. Energy Storage*, vol. 45, p. 103677, Jan. 2022, doi: 10.1016/J.EST.2021.103677.

[2] A. M. Abioye and F. N. Ani, “High Performance Supercapacitor Based on Activated Carbon Electrodes Prepared Using Microwave Temperature as Process Parameter,” pp. 90–95, Dec. 2020, doi: 10.2991/AER.K.201221.017.

[3] J. Zhang, L. Gong, K. Sun, J. Jiang, and X. Zhang, “Preparation of activated carbon from waste Camellia oleifera shell for supercapacitor application,” *J. Solid State Electrochem. 2012 166*, vol. 16, no. 6, pp. 2179–2186, Jan. 2012, doi: 10.1007/S10008-012-1639-1.

[4] Y. F. Ferawati and R. F. Susanti, "The Role of N-Doping to The Pore Characteristics of Activated Carbon from Vetiver Root Distillation Waste," *Metalurgi*, vol. 36, no. 2, pp. 59–68, Sep. 2021, doi: 10.14203/METALURGI.V36I2.595.

[5] Z. Xiao, W. Chen, K. Liu, P. Cui, and D. Zhan, "Porous biomass carbon derived from peanut shells as electrode materials with enhanced electrochemical performance for supercapacitors," *Int. J. Electrochem. Sci.*, vol. 13, no. 6, pp. 5370–5381, Jun. 2018, doi: 10.20964/2018.06.54.

[6] Y. Li and X. Liu, "Activated carbon/ZnO composites prepared using hydrochars as intermediate and their electrochemical performance in supercapacitor," *Mater. Chem. Phys.*, vol. 148, no. 1–2, pp. 380–386, Nov. 2014, doi: 10.1016/J.MATCHEMPHYS.2014.07.058.

[7] R. Chaudhary *et al.*, "Removal of Oil and Grease in Wastewater using Palm Kernel Shell Activated Carbon," *IOP Conf. Ser. Earth Environ. Sci.*, vol. 549, no. 1, p. 012064, Aug. 2020, doi: 10.1088/1755-1315/549/1/012064.

[8] A. Nugroho *et al.*, "Synthesis and Characterization NS-Reduced Graphene Oxide Hydrogel and Its Electrochemical Properties," *Lett. Mater.*, vol. 12, no. 2, pp. 169–174, 2022, doi: 10.22226/2410-3535-2022-2-169-174.

[9] A. N. A. El-Hendawy, "An insight into the KOH activation mechanism through the production of microporous activated carbon for the removal of Pb2+ cations," *Appl. Surf. Sci.*, vol. 255, no. 6, pp. 3723–3730, Jan. 2009, doi: 10.1016/J.APSUSC.2008.10.034.

[10] R. F. Susanti, R. G. R. Wiratmadja, H. Kristianto, A. A. Arie, and A. Nugroho, "Synthesis of high surface area activated carbon derived from cocoa pods husk by hydrothermal carbonization and chemical activation using zinc chloride as activating agent," *Mater. Today Proc.*, 2022.

[11] M. Danish *et al.*, "Comparison of surface properties of wood biomass activated carbons and their application against rhodamine B and methylene blue dye," *Surfaces and Interfaces*, vol. 11, pp. 1–13, Jun. 2018, doi: 10.1016/J.SURFIN.2018.02.001.

[12] R. F. Susanti, A. A. Arie, H. Kristianto, M. Erico, G. Kevin, and H. Devianto, "Activated carbon from citric acid catalyzed hydrothermal carbonization and chemical activation of salacca peel as potential electrode for lithium ion capacitor's cathode," *Ionics 2019 258*, vol. 25, no. 8, pp. 3915–3925, Feb. 2019, doi: 10.1007/S11581-019-02904-X.

[13] K. Byrappa *et al.*, "Impregnation of ZnO onto activated carbon under hydrothermal conditions and its photocatalytic properties," *J. Mater. Sci. 2006 415*, vol. 41, no. 5, pp. 1355–1362, Mar. 2006, doi: 10.1007/S10853-006-7341-X.

[14] A. Nugroho, E. B. Nursanto, S. A. Pradanawati, H. S. Oktaviano, H. Nilasary, and H. Nursukatmo, "Fe based catalysts for petroleum coke graphitization for Lithium Ion battery application," *Mater. Lett.*, vol. 303, p. 130557, 2021, doi: 10.1016/j.matlet.2021.130557.

[15] D. Saramas and S. Ekgasit, "Nano-Zinc Oxide-Doped Activated Carbon from Popped Rice and Its Application for Feed Additive," *Eng. J.*, vol. 25, no. 3, pp. 41–50, Mar. 2021, doi: 10.4186/ej.2021.25.3.41.

[16] S. Ahmed, A. Ahmed, and M. Rafat, "Supercapacitor performance of activated carbon derived from rotten carrot in aqueous, organic and ionic liquid based electrolytes," *J. Saudi Chem. Soc.*, vol. 22, no. 8, pp. 993–1002, Dec. 2018, doi: 10.1016/J.JSCS.2018.03.002.

[17] A. M. Aljeboree and A. B. Mahdi, "Synthesis highly active surface of ZnO/AC nanocomposite for removal of pollutants from aqueous solutions: thermodynamic and kinetic study," *Appl. Nanosci.*, 2021, doi: 10.1007/s13204-021-01946-w.

[18] S. Xiong *et al.*, "Hydrothermal synthesis of high specific capacitance electrode material using porous bagasse biomass carbon hosting MnO2 nanospheres," *Biomass Convers. Biorefinery 2019 114*, vol. 11, no. 4, pp. 1325–1334, Nov. 2019, doi: 10.1007/S13399-019-00525-Y.

[19] Y. Wang *et al.*, "Recent progress in carbon-based materials for supercapacitor electrodes: a review," *J. Mater. Sci. 2020 561*, vol. 56, no. 1, pp. 173–200, Aug. 2020, doi: 10.1007/S10853-020-05157-6.

[20] H. Shen, X. Kong, P. Zhang, X. Song, H. Wang, and Y. Zhang, "In-situ hydrothermal synthesis of δ-MnO2/soybean pod carbon and its high performance application on supercapacitor," *J. Alloys Compd.*, vol. 853, p. 157357, Feb. 2021, doi: 10.1016/J.JALLCOM.2020.157357.

[21] V. Sannasi and K. Subbian, "Influence of Moringa oleifera gum on two polymorphs synthesis of MnO2 and evaluation of the pseudo-capacitance activity," *J. Mater. Sci. Mater. Electron. 2020 3119*, vol. 31, no. 19, pp. 17120–17132, Aug. 2020, doi: 10.1007/S10854-020-04272-Z.